

Supplementary Materials

Modeling Methods

The basic principle of the ATTEC is to enhance the turnover of the POI by tethering the POI to the autophagosome, and thus it is necessary to estimate the turnover rate (or half-life) of the POI and of the POI tethered to the autophagosome. When tethered to the autophagosome, this rate can be estimated by the turnover rate of SQSTM1/p62, an autophagy receptor protein that is mainly degraded by autophagy [1, 2] and has a half-life of ~6 h [3]. Thus, we roughly assumed that the half-life of the POI tethered to the autophagosome is 6 h. To demonstrate the concept of the ATTEC, we showed increased degradation of mutant HTT protein (mHTT) induced by an ATTEC. We used mHTT as the POI for modeling, and its half-life has been reported to be ~33–40 h [4-6]. In order to facilitate calculation, we estimated the mHTT half-life as 36 h, 6 times that of mHTT tethered to autophagosomes.

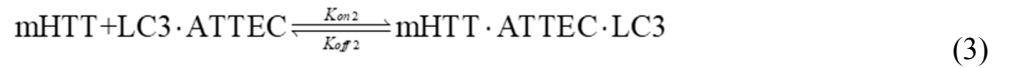
Besides the turnover rates, we also needed to estimate the starting concentrations of the POI and LC3 before compound treatment. It has been estimated that cells have 2–4 million (median, 3 million) protein molecules per cubic micron^[7]. In addition, our previous proteomics data showed that the fractions of total HTT (including both mutant and wild-type HTT) and LC3 are 1/100,000 and 6/100,000 of total protein, respectively [8]. Based on the above information, we estimated that the starting concentrations of intracellular mHTT and LC3 were 33 and 400 nmol/L, respectively.

In addition to the estimation of these biological parameters, we made some assumptions to further simplify the model. First, we assumed that the LC3 level remained constant during the process of drug treatment. This was reasonable because experimental data showed that neither the LC3-I nor the LC3-II levels were influenced by ATTEC treatment [8]. In addition, it was consistent with the fact that LC3 is an abundant protein with a fast turnover rate [9, 10]. We also assumed that the total levels of ATTEC remained

constant. We recognize that this assumption is over-simplified. Meanwhile, it is reasonable, since the culture medium was changed every day during experiments, which replenished the potential loss of the compound due to degradation or metabolic changes. In addition, the experimental degradation rate of the compounds in free and in protein-bound forms were extremely difficult to determine and may have added a major layer of complexity to our model. Thus, we focused on the target protein degradation only and assumed a constant level of the compounds in cell culture.

Finally, to simplify the model, we assumed that the binding of the ATTEC to one protein did not influence its binding to the other, i.e., the LC3-bound ATTEC and free ATTEC had the same affinity for mHTT, and the mHTT-bound ATTEC and free ATTEC had the same affinity for LC3. We made this assumption to simplify the model, which could be modified if additional evidence reveals a positive or negative coupling between the binding of the two proteins to ATTEC.

We used the following chemical reactions for modeling,



where the K_{on1} and K_{off1} are the association and dissociation rate constants of LC3 binding to the mHTT-bound ATTEC and free ATTEC, respectively; K_{on2} and K_{off2} are the association and dissociation rate constants of the mHTT binding to LC3-bound ATTEC and free ATTEC, respectively.

Based on the above chemical reactions and the assumptions noted, the kinetic equations were written as,

$$\frac{d[\text{LC3} \cdot \text{ATTEC}]}{dt} = K_{on1}[\text{LC3}][\text{ATTEC}] - K_{off1}[\text{LC3} \cdot \text{ATTEC}]$$

$$-K_{on2}[LC3 \cdot ATTEC][mHTT] + K_{off2}[mHTT \cdot ATTEC \cdot LC3] \quad (5)$$

$$\begin{aligned} \frac{d[ATTEC \cdot mHTT]}{dt} = & K_{on2}[mHTT][ATTEC] - K_{off2}[ATTEC \cdot mHTT] \\ & -K_{on1}[ATTEC \cdot mHTT][LC3] + K_{off1}[mHTT \cdot ATTEC \cdot LC3] \\ & - \frac{\ln 2}{36} [ATTEC \cdot mHTT] \end{aligned} \quad (6)$$

$$\begin{aligned} \frac{d[mHTT \cdot ATTEC \cdot LC3]}{dt} = & K_{on2}[LC3 \cdot ATTEC][mHTT] - K_{off2}[mHTT \cdot ATTEC \cdot LC3] \\ & + K_{on1}[ATTEC \cdot mHTT][LC3] - K_{off1}[mHTT \cdot ATTEC \cdot LC3] \\ & - \frac{\ln 2}{36} [mHTT \cdot ATTEC \cdot LC3] - \frac{\ln 2}{6} [mHTT \cdot ATTEC \cdot LC3] \end{aligned} \quad (7)$$

$$\frac{d([ATTEC] + [ATTEC \cdot mHTT] + [LC3 \cdot ATTEC] + [mHTT \cdot ATTEC \cdot LC3])}{dt} = 0 \quad (8)$$

$$\frac{d([LC3] + [LC3 \cdot ATTEC] + [mHTT \cdot ATTEC \cdot LC3])}{dt} = 0 \quad (9)$$

$$\begin{aligned} \frac{d([mHTT] + [ATTEC \cdot mHTT] + [mHTT \cdot ATTEC \cdot LC3])}{dt} = & \frac{\ln 2}{36} [mHTT]_{t=0} - \frac{\ln 2}{36} [mHTT] \\ & - \frac{\ln 2}{36} [ATTEC \cdot mHTT] - \frac{\ln 2}{36} [mHTT \cdot ATTEC \cdot LC3] - \frac{\ln 2}{6} [mHTT \cdot ATTEC \cdot LC3] \end{aligned} \quad (10)$$

Eq. (5) is based on the kinetics of chemical reactions (1) and (3), while Eq. (6) is based on the kinetics of reactions (2) and (4), as well as the degradation of the binary complex ATTEC·mHTT, which was assumed to be degraded at the same rate as free mHTT with a half-life of 36 h. Note that the binary complexes participate in not only the reactions between free protein and free ATTEC [reactions (1) and (2)], but also the reactions to form ternary complexes [reactions (3) and (4)]. Similarly, Eq. (7) is based on the kinetics of reactions (3) and (4), as well as the degradation of the ternary complex, which was subject to both ATTEC-induced autophagic degradation with an estimated half-life of 6 h and endogenous degradation with an estimated half-life of 36 h. The concentration of the ternary complex increased with

binary complex association and decreased with ternary complex dissociation as well as its degradation. Eq. (8) and Eq. (9) are based on the assumption that the total concentration of LC3 and ATTEC remained constant over time. Eq. (10) is based on the protein synthesis rate and degradation of several different mHTT-containing species. The mHTT was synthesized over time, and the synthesis rate was determined by the level of mutant *HTT* mRNA and the protein translation rate. These were not changed by the ATTEC, which only targeted the mutant *HTT* protein but not mRNA to autophagic degradation. Thus, the protein synthesis rate would remain constant, which could be estimated by the fact that the mHTT remained at steady-state level before ATTEC treatment. Thus, based on the equilibrium of mHTT protein synthesis and degradation, the synthesis rate could be calculated by the mHTT half-life (36 h) and its starting concentration ($[mHTT]_{t=0}$) to be $\frac{\ln 2}{36} [mHTT]_{t=0}$. Similarly, the degradation of total mHTT by endogenous the degradation system (independent of the ATTEC) was calculated based on a half-life of 36 h, but the degradation rates are proportional to the real-time concentrations of each individual species. Thus, the ATTEC-independent degradation rate of total mHTT is equal to $\frac{\ln 2}{36} [mHTT] + \frac{\ln 2}{36} [ATTEC \cdot mHTT] + \frac{\ln 2}{36} [mHTT \cdot ATTEC \cdot LC3]$. In addition, the ternary complex mHTT·ATTEC·LC3 was degraded by ATTEC-induced autophagic degradation, which was estimated to have a half-life of 6 h and accounted for the $\frac{\ln 2}{6} [mHTT \cdot ATTEC \cdot LC3]$ component in Eq. (10). Note that a minus sign was added to each degradation component to indicate a decrease of concentration over time.

In order to simulate and understand the dose-dependence curves of ATTEC-induced mHTT lowering, we calculated the total mHTT level at different compound concentrations based on the steady-state equations shown below:

$$\begin{aligned}
 &K_{on1}[LC3][ATTEC] - K_{off1}[LC3 \cdot ATTEC] \\
 &-K_{on2}[LC3 \cdot ATTEC][mHTT] + K_{off2}[mHTT \cdot ATTEC \cdot LC3] = 0
 \end{aligned} \tag{11}$$

$$\begin{aligned}
& K_{on2}[\text{mHTT}][\text{ATTEC}] - K_{off2}[\text{ATTEC} \cdot \text{mHTT}] \\
& -K_{on1}[\text{ATTEC} \cdot \text{mHTT}][\text{LC3}] + K_{off1}[\text{mHTT} \cdot \text{ATTEC} \cdot \text{LC3}] \\
& - \frac{\ln 2}{36} [\text{ATTEC} \cdot \text{mHTT}] = 0
\end{aligned} \tag{12}$$

$$\begin{aligned}
& K_{on2}[\text{LC3} \cdot \text{ATTEC}][\text{mHTT}] - K_{off2}[\text{mHTT} \cdot \text{ATTEC} \cdot \text{LC3}] \\
& + K_{on1}[\text{ATTEC} \cdot \text{mHTT}][\text{LC3}] - K_{off1}[\text{mHTT} \cdot \text{ATTEC} \cdot \text{LC3}] \\
& - \frac{\ln 2}{36} [\text{mHTT} \cdot \text{ATTEC} \cdot \text{LC3}] - \frac{\ln 2}{6} [\text{mHTT} \cdot \text{ATTEC} \cdot \text{LC3}] = 0
\end{aligned} \tag{13}$$

$$[\text{ATTEC}] + [\text{ATTEC} \cdot \text{mHTT}] + [\text{LC3} \cdot \text{ATTEC}] + [\text{mHTT} \cdot \text{ATTEC} \cdot \text{LC3}] = [\text{ATTEC}]_{t=0} \tag{14}$$

$$[\text{LC3}] + [\text{LC3} \cdot \text{ATTEC}] + [\text{mHTT} \cdot \text{ATTEC} \cdot \text{LC3}] = [\text{LC3}]_{t=0} \tag{15}$$

$$\ln 2 \left(\frac{[\text{mHTT}]_{t=0}}{36} - \frac{[\text{mHTT}]}{36} - \frac{[\text{ATTEC} \cdot \text{mHTT}]}{36} - \frac{[\text{mHTT} \cdot \text{ATTEC} \cdot \text{LC3}]}{36} - \frac{[\text{mHTT} \cdot \text{ATTEC} \cdot \text{LC3}]}{6} \right) = 0 \tag{16}$$

Eqs (11), (12), and (13) are based on the kinetic equations (5) through (7), while Eqs (14) and (15) are based on the assumption that the total ATTEC and total LC3 concentrations remain constant. For steady-state, the total mHTT reaches an equilibrium level, and this is described by Eq. (16).

References

- [1] Johansen T, Lamark T. Selective autophagy mediated by autophagic adapter proteins. *Autophagy* 2011, 7: 279-296.
- [2] Myeku N, Figueiredo-Pereira ME. Dynamics of the degradation of ubiquitinated proteins by proteasomes and autophagy: association with sequestosome 1/p62. *J Biol Chem* 2011, 286: 22426-22440.

- [3] Bjorkoy G, Lamark T, Brech A, Outzen H, Perander M, Overvatn A, *et al.* p62/SQSTM1 forms protein aggregates degraded by autophagy and has a protective effect on huntingtin-induced cell death. *J Cell Biol* 2005, 171: 603-614.
- [4] Tsvetkov AS, Arrasate M, Barmada S, Ando DM, Sharma P, Shaby BA, *et al.* Proteostasis of polyglutamine varies among neurons and predicts neurodegeneration. *Nat Chem Biol* 2013, 9: 586-592.
- [5] Wu P, Lu MX, Cui XT, Yang HQ, Yu SL, Zhu JB, *et al.* A high-throughput-compatible assay to measure the degradation of endogenous Huntingtin proteins. *Acta Pharmacol Sin* 2016, 37: 1307-1314.
- [6] Fu Y, Wu P, Pan Y, Sun X, Yang H, Difiglia M, *et al.* A toxic mutant huntingtin species is resistant to selective autophagy. *Nat Chem Biol* 2017, 13: 1152-1154.
- [7] Milo R. What is the total number of protein molecules per cell volume? A call to rethink some published values. *Bioessays* 2013, 35: 1050-1055.
- [8] Li Z, Wang C, Wang Z, Zhu C, Li J, Sha T, *et al.* Allele-selective lowering of mutant HTT protein by HTT-LC3 linker compounds. *Nature* 2019, 575: 203-209.
- [9] Ni HM, Bockus A, Wozniak AL, Jones K, Weinman S, Yin XM, *et al.* Dissecting the dynamic turnover of GFP-LC3 in the autolysosome. *Autophagy* 2011, 7: 188-204.
- [10] Moulis M, Vindis C. Methods for Measuring Autophagy in Mice. *Cells* 2017, 6.

Supplementary Figures

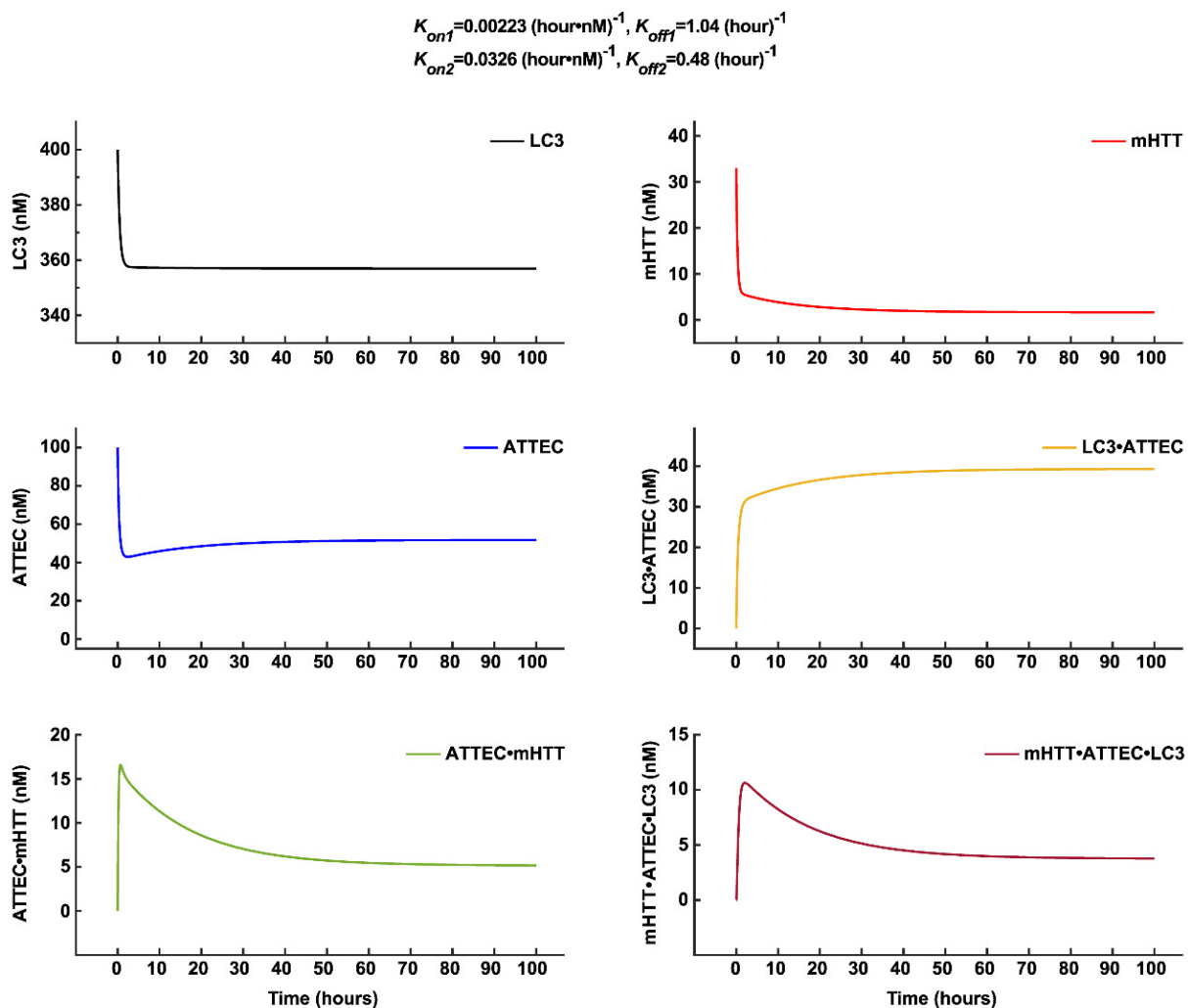


Fig. S1 Kinetic modeling of the indicated species involved in the ATTEC

The simulated concentrations of each of the indicated species over time. The species are the free LC3 protein (LC3), the free mHTT (mHTT), the free ATTEC (ATTEC), the LC3·ATTEC binary complex (LC3·ATTEC), the ATTEC·mHTT binary complex (ATTEC·mHTT), and the mHTT·ATTEC·LC3 ternary complex (mHTT·ATTEC·LC3). The kinetics parameters used for modeling are presented above the panels. The ATTEC concentration for modeling is 100 nmol/L.

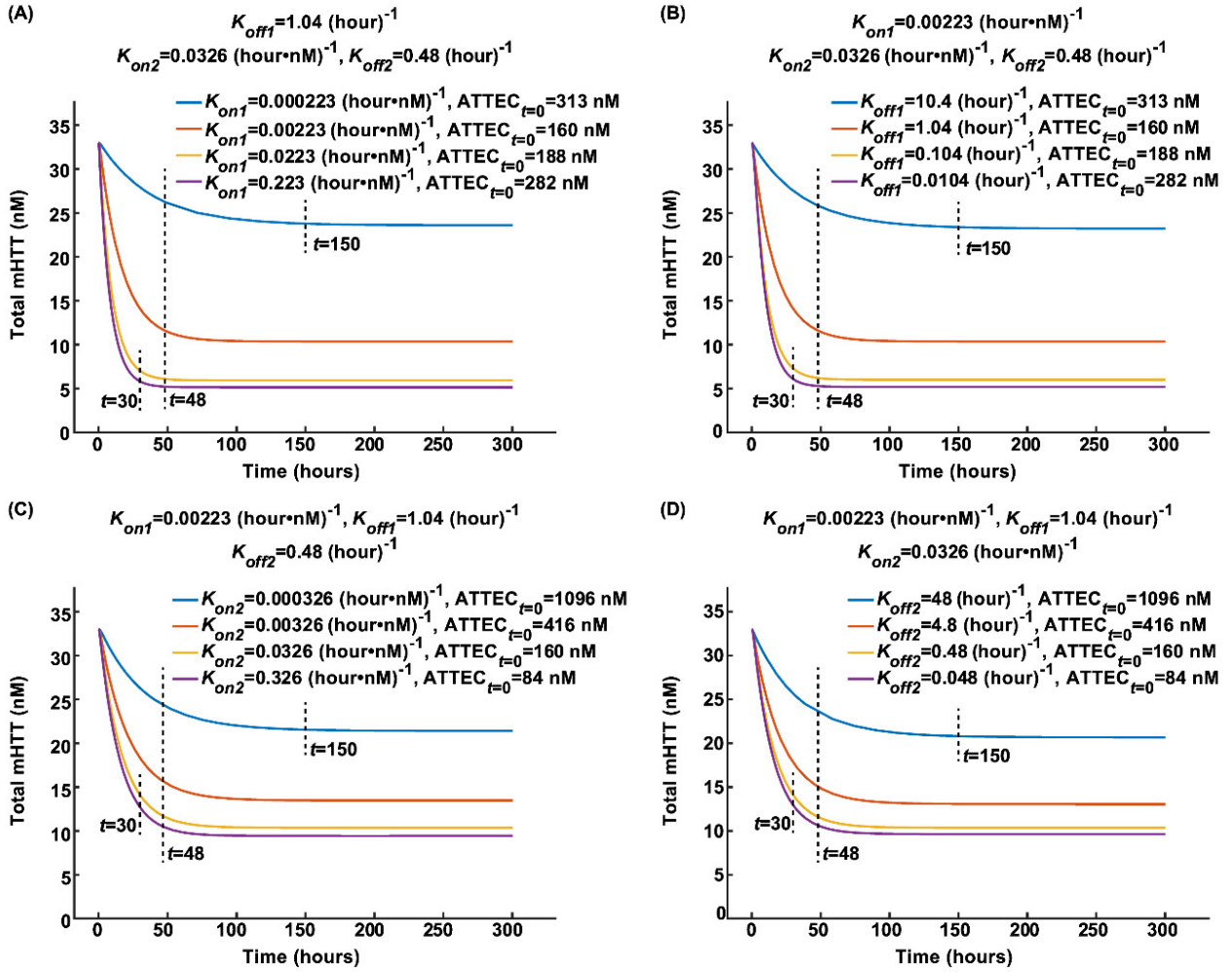


Fig. S2 Kinetic modeling of the total mHTT concentrations

A Simulated total mHTT concentration–time relationship with the indicated set of K_{on1} values when K_{off1} , K_{on2} , and K_{off2} are fixed. **B** Similar to **A**, but with the indicated set of K_{off1} values when fixing all other kinetic parameters. **C** Similar to **A**, but with the indicated set of K_{on2} values when fixing all other kinetic parameters. **D** Similar to **A**, but with the indicated set of K_{off2} values when fixing all other kinetic parameters. Note that the ATTEC concentrations used for each simulation are the optimal concentrations to achieve the highest D_{max} under each condition (see Fig. 4). The dashed lines indicate the time needed to reach steady-state levels.

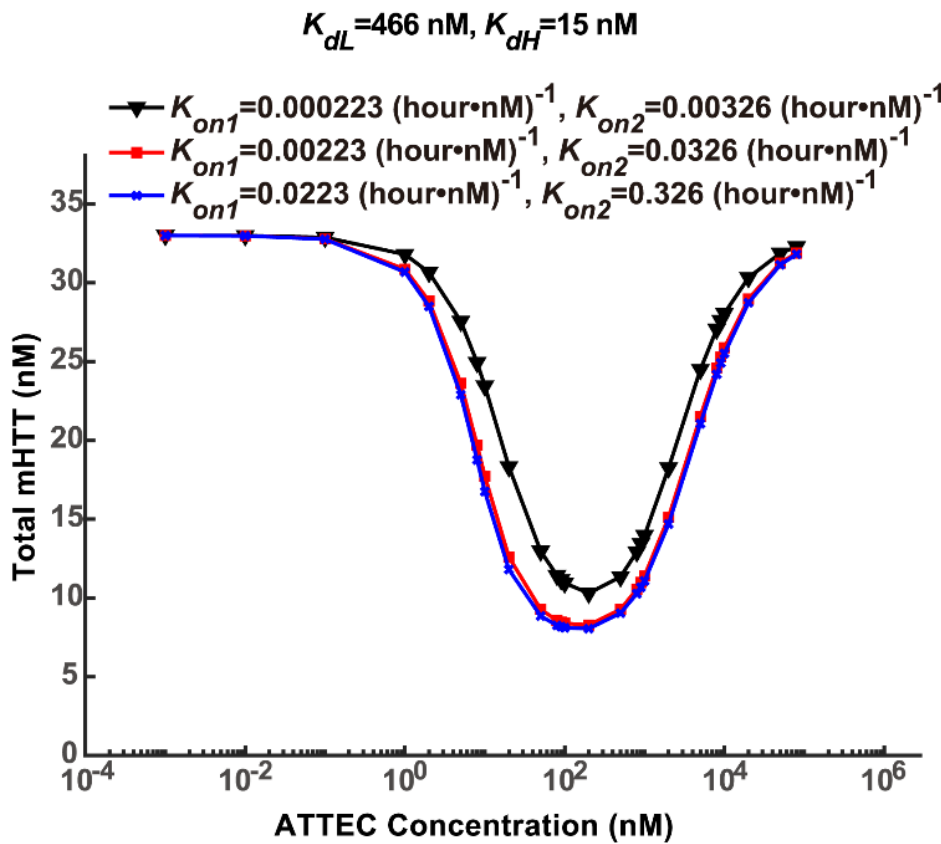


Fig. S3 Modeling the dose-dependence curves for the ATTEC with fixed K_d values. Simulated relationship between the steady-state concentrations of total mHTT and the concentrations of ATTEC molecules with fixed K_{dH} and K_{dL} by varying K_{on1} , K_{off1} , K_{on2} , and K_{off2} accordingly. The K_{dH} and K_{dL} values are set to the experimental values of GW5074, one of our previously-identified ATTECs.

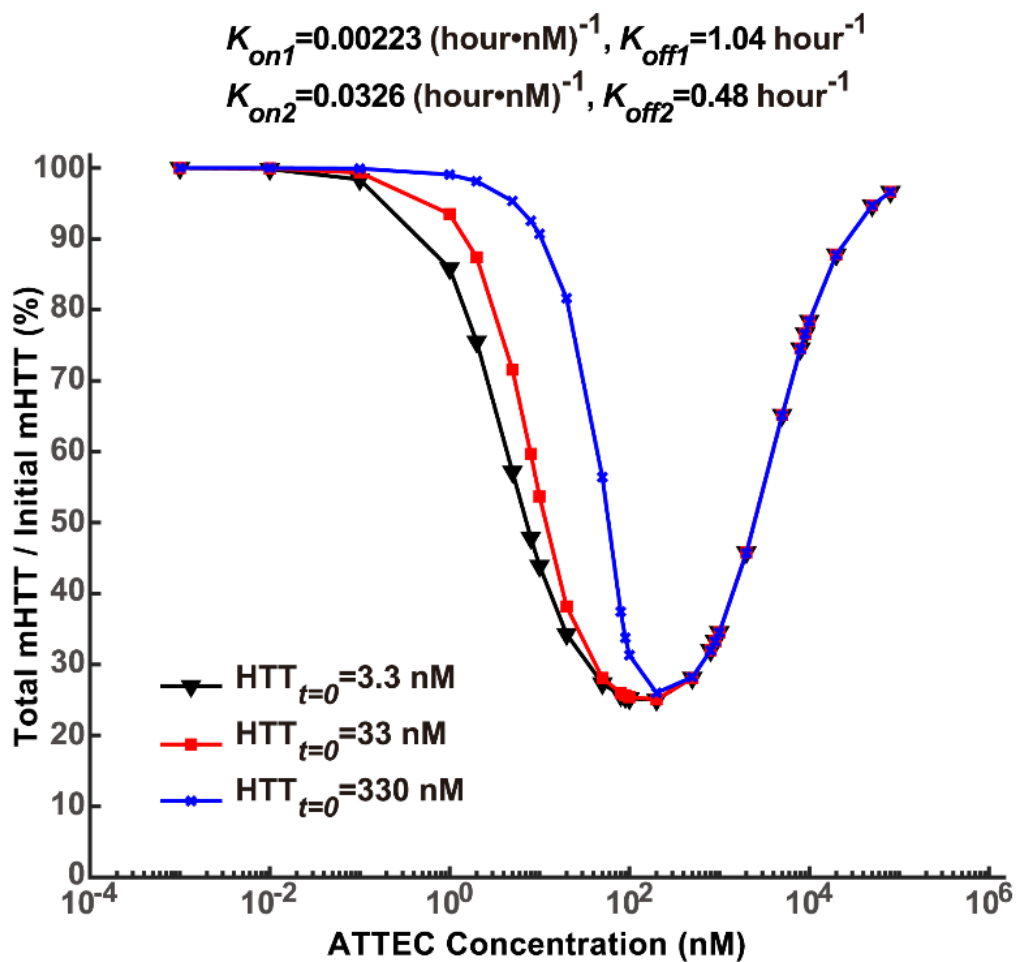


Fig. S4 Modeling the dose-dependence curves for the ATTEC with different mHTT initial concentrations. Simulated relationship between the percentage of mHTT degradation and the concentrations of the ATTEC with fixed K_{on1} , K_{off1} , K_{on2} , and K_{off2} by varying initial mHTT concentrations.